Biomedical Materials

PAPER

Evaluation of different methodologies for primary human dermal fibroblast spheroid formation: automation through 3D bioprinting technology

Cristina Quílez[1,5], Enrique Cerdeira[2,5], Jorge González-Rico[3], Gonzalo de Aranda[1], Maria Luisa López-Donaire[3], José Luis Jorcano[1,4] and Diego Velasco[1,4,*]

[1] Department of Bioengineering and Aerospace Engineering, Universidad Carlos III de Madrid, Leganés, Spain
[2] BIST Dolors Aleu Graduate Centre, Universitat Pompeu Fabra (UPF), Barcelona, Spain
[3] Department of Continuum Mechanics and Structural Analysis, Universidad Carlos III de Madrid, Leganés, Spain
[4] Instituto De Investigacion Sanitaria Gregorio Marañon, Madrid, Spain
[5] These authors contributed equally to this work.
[*] Author to whom any correspondence should be addressed.

E-mail: divelasc@ing.uc3m.es

Keywords: cell spheroids, primary human dermal fibroblasts (dHFs), U-shape low adhesion plate, 3D bioprinting, viscosity enhancer, hyaluronic acid, glycerol

Supplementary material for this article is available online

OPEN ACCESS

RECEIVED
18 March 2022

REVISED
27 May 2022

ACCEPTED FOR PUBLICATION
14 June 2022

PUBLISHED
1 July 2022

Abstract

Cell spheroids have recently emerged as an effective tool to recapitulate native microenvironments of living organisms in an *in vitro* scenario, increasing the reliability of the results obtained and broadening their applications in regenerative medicine, cancer research, disease modeling and drug screening. In this study the generation of spheroids containing primary human dermal fibroblasts was approached using the two-widely employed methods: hanging-drop and U-shape low adhesion plate (LA-plate). Moreover, extrusion-based three-dimensional (3D) bioprinting was introduced to achieve a standardized and scalable production of cell spheroids, decreasing considerably the possibilities of human error. This was ensured when U-shape LA-plates were used, showing an 85% formation efficiency, increasing up to a 98% when it was automatized using the 3D bioprinting technologies. However, sedimentation effect within the cartridge led to a reduction of 20% in size of the spheroid during the printing process. Hyaluronic acid (HA) was chosen as viscosity enhancer to supplement the bioink and overcome cell sedimentation within the cartridge due to the high viability values exhibited by the cells—around 80%—at the used conditions. Finally, (ANCOVA) of spheroid size over time for different printing conditions stand out HA 0.4% (w/v) 60 kDa as the viscosity-improved bioink that exhibit the highest cell viability and spheroid formation percentages. Besides, not only did it ensure cell spheroid homogeneity over time, reducing cell sedimentation effects, but also wider spheroid diameters over time with less variability, outperforming significantly manual loading.

1. Introduction

Spheroids are cell aggregates constituted through self-assembly in suspension. Contrary to conventional monolayer cultures, these culture systems provide cells with three-dimensional (3D) microenvironmental cues that resemble closely physicochemical *in vivo* conditions and architecture [1–3]. They remove the unnatural effects of cell adhesion onto planar surfaces and, instead, preserve both cultured cells phenotype as well as biochemical pathways involved in cell-to-cell or cell-to- extracellular matrix (ECM) interactions, so that they can be fully exploited *in vitro* [4], being particularly useful in cancer research and drug discovery. Unlike traditional 2D cultures, cell spheroids represent a more realistic and predictive platform for biomedical research purposes as there exists no constraint for the span of multi-cellular functions and interactions that can be recapitulated within a 3D framework [5]. This culture

methodology has been broadly explored for *in vitro* modeling of different diseases [2, 6–8], especially for *in vitro* tumor models in cancer studies, for either one cell population or mixed cell populations. Of particular interest is the use of human primary dermal fibroblasts spheroid culture, which has been widely explored to be used as dermal models to test skin care products [9, 10], to improve wound healing [11], to be used in aging treatments [12] and to model skin fibrosis and keloids [13].

Spheroid formation has been described using different methodologies [14–16], which include hanging-drop (HD), spinner culture, microfluidics or the use of hydrogels to avoid cell adhesion to the substrate. The HD methodology has been extensively reported in the literature thanks to the low requirement of expensive or professional equipment in small scale experiments [17–19]. However, specific spheroid culture plates with low-adherence U-shaped surface that promote cell aggregation have emerged as an alternative with high reproducibility [20, 21]. Although this culture system enables the production of 96 spheroids in each plate, it involves manual loading of the cells, being this a time-consuming process that could lead to human error. Three-dimensional bioprinting has risen as a powerful technique to automate and scale tissue production *in vitro* [22, 23]. On the whole, this groundbreaking technology contributes to increased yield, reduction in costs and product standardization. More recently, this technology has been widely applied in the generation of cellular spheroids to build tumor models [24, 25]. For this reason, most of the articles regarding spheroid bioprinting mostly involve extrusion-based bioprinting [26, 27], with laser-based bioprinting used to a minor extent [28, 29]. Regardless the printing methodology, when cells are included inside the bioink, gravity-driven cell sedimentation within the extrusion syringe in low-density bioinks arises as a limitation during the fabrication process [30, 31]. To overcome this limitation, viscosity enhancers are secondary biomaterials that are added to the bioink to improve the viscosity of the printed solution, conferring strength and cohesion to maintain shape fidelity and preserve printing resolution. With this purpose, biocompatible materials like hyaluronic acid (HA) have been used to supplement bioinks primarily in extrusion-based bioprinting and obtain 3D constructs [32, 33]. Simultaneously, other viscous inorganic substances such as glycerol have shown a great potential to control cell sedimentation [34].

In this work, different methods for the fabrication of human dermal fibroblast (dHF) spheroids have been studied. With this purpose, two different and widely used manual fabrication methods—HD and commercial low-adhesion (LA) culture plates—were analyzed and compared in terms of formation efficiency and spheroid morphology. Additionally, we have evaluated whether the presence of antibiotics (ABs) and antimycotics (AMs) during cell culture affect spheroid formation efficiency [35]. However, the paramount objective of this work was to achieve cell spheroid fabrication in an automated and scalable way based on extrusion 3D bioprinting approach. In doing so, different printing conditions were evaluated (feed rate and viscosity condition of the bioink) to elucidate which of them accomplished homogeneous and mass production of cell spheroids by reducing cell sedimentation over time. Additionally, this research intended to assess whether viscosity-enhanced solutions posed a risk to cell safety or hindered spheroid assembly with a view to ensuring viability of the spheroids in further applications.

2. Materials and methods

2.1. Cell culture

Primary dHFs from commercial origin (PromoCell, Heidelberg, Germany) were maintained in liquid nitrogen prior to use. Cells were defrosted and seeded following manufacturer's instructions and cultured in Dulbecco's modified Eagle's medium (DMEM) containing 10% fetal bovine serum (FBS) and 1% AB-AM (ThermoFisher, Waltham, MA, USA). For culture conditions without AB-AM, cells were cultured at least for 48 h with culture media without AB-AM. Cells were cultured at 37 °C, 80% humidity and 5% CO_2 until they reached at 80% confluency, point at which they were detached for further use.

2.2. Manual spheroid formation

For spheroid generation, two different methods were evaluated: HD and LA U-shape culture plate specific for spheroid cell culture (LA-plate). HD culture was based on the methods described in detail by Topouzi *et al* [36]. Briefly, when cell culture was at 80% confluency, cells were detached and resuspended at a cell density of 300 cells μl^{-1} in DMEM/10% FBS w/o 1% AB-AM. For spheroid formation, 10 µl drop of the cell suspension was deposited on the lid of a 100 mm culture plate. The culture plate was filled with 1X phoshate-buffered saline (PBS) and covered with the lid containing the hanging drops (figure 1(a)). Additionally, to avoid cell culture evaporation, a 100 mm culture plate filled with PBS 1X was stacked on top of the plate containing the drops. Cell culture plates were incubated 48 h at 37 °C and 5% CO_2 to allow spheroid formation. For each condition, at least 50 spheroids were generated, each containing 3000 cells.

To compare spheroid formation methods, spheroids were also generated using LA-plates specific for spheroid cell culture (faCellitate, Mannheim, Germany). For this purpose, 10 µl of the cell suspension was introduced in each well and supplemented with 100 µl of culture media (DMEM/10% FBS/1% AB-AM). Culture plates were placed on an incubator

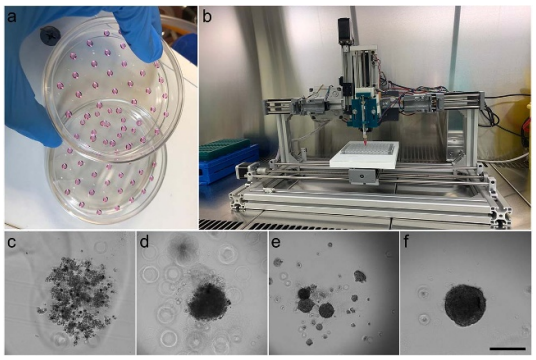

Figure 1. Spheroid formation using (a) HD method and (b) 3D bioprinting using LA-plate. Example of different structures found after formation and their classification as spheroid or no-spheroid: (c) no-spheroid as there was a cell dispersion with no aggregation; (d) no-spheroid as there was no clear borders in the aggregation; (e) no-spheroid due to the presence of multiple aggregations and (f) spheroid. Scale bar: 300 μm.

for 48 h at 37 °C and 5% CO_2 for spheroid formation. For each condition, at least 50 spheroids were generated.

2.3. Automatized spheroid formation

The *in-house* extrusion bioprinter is composed of two main parts: a fixed extrusion module and a mobile printing bed (figure 1(a)). The extrusion module comprises four electric stepper motors and four sterile syringes. For small-volume release, two different positioners with 10 μl gastight glass-syringes (SGE, Melbourne, Australia) were placed vertically and perpendicular to the printing bed which moves in the *z*-axis for direct bioink extrusion onto the culture plate. The printing bed holds the culture plate and moves in the *x*–*y*-axes for precise positioning driven by two electric stepper motors. For bioink preparation, cell suspension containing 300 cells μl^{-1} in DMEM/10% FBS/1% AB-AM was introduced in a 10 μl gastight glass-syringe with a 22G PTFE-coated dispensed tip (Nordson, Westlake, OH, USA) that controls wicking to stop dripping. To analyze the effect of the culture plate used, bioprinting was performed using both HD method and LA-plate. With that purpose, 10 μl bioink solution was extruded in either the lid of a 100 mm culture plate or in each well of a LA-plate with a flow of 3 μl s^{-1}. Then, for LA-plate, each well is supplemented with extra 100 μl of cell culture medium. Cell culture plates were incubated 48 h at 37 °C and 5% CO_2 to allow spheroid formation, each containing 3000 cells. To analyze the effect of printing velocity on spheroid formation, two different velocities (feed rates) were used: 9 and 6 wells min^{-1}.

2.4. Viscosity enhancer solutions study

To avoid cell seeding during bioprinting, glycerol (Sigma Aldrich, San Luis, MO, USA) and HA (Life Core Biomedical, Chaska, MN, USA) were evaluated as potential viscosity enhancers. For the selection of the correct material and concentration, both viability and formation efficiency were analyzed. LA-plate was selected as the suitable method for spheroid bioprinting (see section 3.1), reason why all the analysis of viscosity enhancer solutions were performed using this methodology.

2.4.1. Cell viability analysis

Different concentration of glycerol and HA were evaluated to produce various degrees of viscosity. For glycerol, 1%, 10%, 50% and 90% (v/v) solutions were prepared in DMEM/10% FBS/1% AB-AM culture medium. On the other hand, different molecular weights of HA were tested (60, 200, 500 and 700 kDa and 1 MDa) for a constant concentration of HA (1% (w/v)) prepared in DMEM/10% FBS/1% AB-AM culture media. All solutions were stirred overnight. For cell dHFs culture, 10 000 cells $well^{-1}$ were plated into a 96-well plate and incubated overnight at 37 °C, 80% humidity and 5% CO_2. Then 100 μl of viscosity enhancer solutions were added to each well ($n = 8$ per condition) and cultured overnight at 37 °C, 80% humidity and 5% CO_2 to proceed with the viability assays.

AlamarBlue (Invitrogen, Paisley, Scotland) working solution was prepared at 10% (v/v) according to manufacturer's instructions diluted in DMEM/10% FBS/1% AB-AM culture medium. Following, 100 μl of AlamarBlue working solution was added to each well and incubated 3 h at 37 °C, 80% humidity and 5% CO_2. Finally, the absorbance (450 nm) was measured in a Synergy HTX multi-mode reader (Biotek, Winooski, VT, USA).

Live/Dead® (Invitrogen, Paisley, Scotland) working solution was prepared in PBS 1X by the addition of Calcein-AM and EthD-1 in a final concentration of 2 μM each. Following manufacturer's protocol, 100 μl of Live/Dead® working solution was added to each well and incubated 1 h at 37 °C, 80% humidity and 5% CO_2 to proceed with image acquisition under the DMi8 Leica microscope (Leica Microsystems, Wetzlar, Germany). For each condition three samples were analyzed. Viability was quantified using ImageJ software and expressed as:

$$\text{Viability } (\%) = n_l/n_d + n_l$$

where n_l and n_d are the number of live (green fluorescence) and dead (red fluorescence) cells respectively.

2.4.2. Manual formation of spheroids using viscosity enhancer solutions

To analyze the effect that viscosity enhancer on spheroid formation, spheroids containing 3000 were manually generated using LA-plate in the presence of HA and glycerol at different concentrations. With that purpose, 1%, 10% (v/v) glycerol solutions and 0.1%,

0.4% and 0.8% (w/v) HA (60, 200 and 500 kDa) solutions were prepared in DMEM/10% FBS/1% AB-AM culture medium [37]. Spheroids were manually generated as described in section 2.2, using the viscosity enhancer solutions to resuspend the cells. Cells resuspended in culture media without viscosity enhancer were used as a control.

2.4.3. Determination of bioink viscosity

Rheological properties of the solutions were evaluated at room temperature using a TA HR-20 rheometer from Waters TA Q600 (TA instrument, New Castle, DE, USA) equipped with a parallel plate geometry (stainless steel, 40 mm plate diameter). Viscosity was evaluated by a steady flow measurement through a shear rate sweep from 1 to 1000 s^{-1} followed by a second sweep from 1000 to 1 s^{-1}. With that purpose, 1%, 10% (v/v) glycerol solutions and 0.1%, 0.4% and 0.8% (w/v) HA (60, 200 and 500 kDa) solutions were prepared in DMEM/10% FBS/1% AB-AM culture medium. Given a printing flow of 3 µl s^{-1}, viscosity was represented within the first decade (shear rate 10–100 Pa) [38].

2.4.4. Automatized spheroid formation using viscosity enhancer solution

To analyze the effect of viscosity enhancer in spheroid formation, spheroid containing 3000 cells were generated using the bioprinter as described in section 2.3. For that, viscosity enhancer solutions containing 0.4% HA (60, 200 and 500 kDa) were prepared in DMEM/10% FBS/1% AB-AM culture medium to be used as bioink. Cells resuspended in culture media without viscosity enhancer were used as a control.

2.5. Data acquisition and analysis

After spheroid formation, images of each spheroid were taken using a calibrated inverted microscope Olympus CKX41 (Olympus Lifesciences, Tokyo, Japan) with PixeLINK camera with a 10× magnification. At least 50 images of each condition were taken in tagged image file format (.tiff) for formation efficiency and morphometric analysis. To track the effect of cell seeding over time, pictures were taken in the same order as the spheroids were generated. In order to analyze the effect of different culture conditions in formation efficiency, first, images were classified as spheroid/no-spheroid according to the following criteria: spheroids were circular and with clearly defined borders. Additionally, the effect of different culture conditions in spheroid size and morphology was studied by analyzing spheroid diameter and roundness. A self-designed program in MATLAB (MathWorks, Natik, MA, USA) available in the group was used to extract the area and roundness of each spheroid.

2.6. Statistical analysis

Statistical analysis was performed using R-Studio software (RStudio PBC, Boston, MA, USA). Chi-squared test (χ^2-test) of independence was used to test whether spheroid formation was influenced by any culture condition or fabrication method [39]. The independence of variables (H0) was tested with a significance level of 0.05. Additionally, the effect of culture condition in either cell diameter or roundness was tested independently. Equality of means (H0) was tested for a significance level of 0.05 with one-way analysis of variance (ANOVA) to analyze whether each culture condition influenced spheroid diameter. Additionally, Tukey's test was used to investigate multiple relations for explanatory variables with multiple levels [40]. Finally, to evaluate the effect that the combined interaction of printing condition and time on spheroid diameter had, equality of slopes (H0) was tested for a significance level of 0.05 with analysis of covariance (ANCOVA) test [41, 42]. This statistical compares the mean values of a response variable present in two or more samples according to a categorical variable known as factor while taking into consideration the effect of a metric independent variable known as covariate. In doing so, it evaluated the similarity between the regression lines of each pair of experiments by testing the effect that the categorical variable *culture condition* had on the response variables of *diameter* while factoring the influence of the continuous and independent covariable of *time* into the analysis.

3. Results

3.1. Manual spheroid formation

To analyze the effect of different culture conditions in spheroid formation efficiency, first, spheroids were manually generated using both HD method and LA culture plates specific for spheroid formation. After 48 in culture, spheroids were visually inspected and classified as non-spheroids (figures 1(c)–(e)) or spheroid (figure 1(f)). The effect that the presence of antibiotic/antimycotic (AB-AM) has on spheroid formation and morphology was first analyzed in HD method. Chi-squared analysis of formation efficiency report that manual spheroid formation using HD method was not affected by the presence or the absence of AB-AM (figure 2(a)). Although in the absence of AB-AM formation efficiency was slightly higher −80% with respect a 75%, it showed a wider distribution. Moreover, spheroid size showed a mean value of 180 µm, both in the presence or the absence of AB-AM in HD method, with no significant difference in spheroid roundness (figure 3(b) and supplementary 1).

From this point on, cell cultures were maintained in the presence of AB-AM to proceed with the rest of studies.

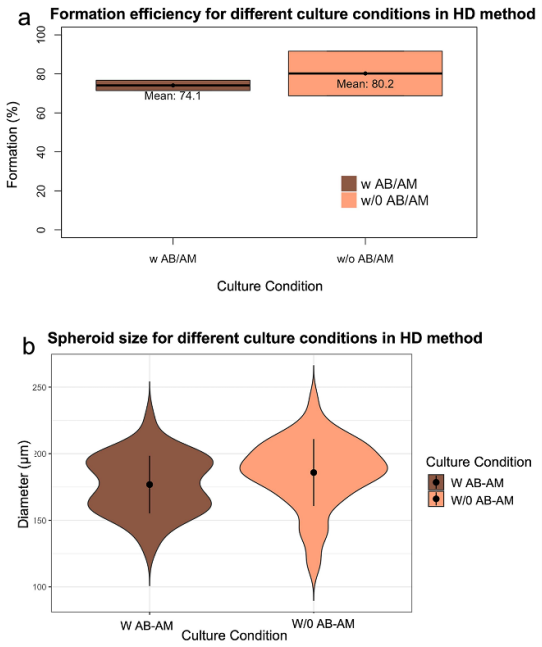

Figure 2. (a) Boxplot of formation efficiency in the presence or absence of AB-AM using HD method and (b) violin plot representing spheroid size analysis in presence or absence of AB-AM in HD method. Statistical significance: p-value < 0.05*, p-value < 0.01** and p-value < 0.001***.

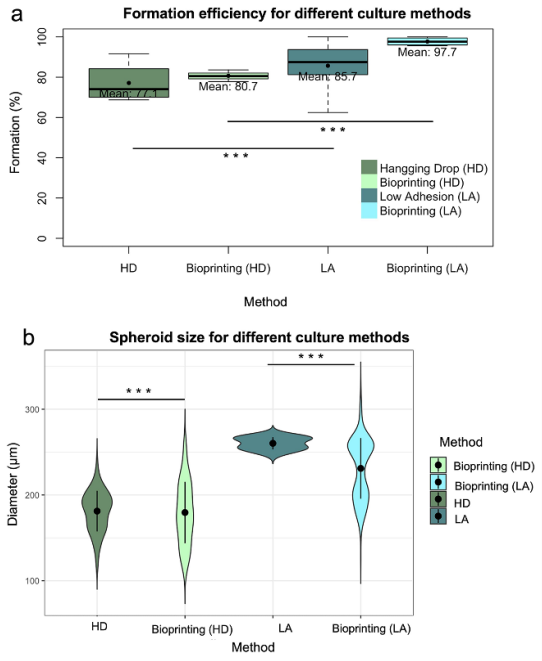

Figure 3. (a) Boxplot of formation efficiency for different formation methods in the presence of AB-AM (b) violin plot representing spheroid size analysis for different formation methods. Statistical significance: p-value < 0.05*, p-value < 0.01** and p-value < 0.001***.

Regarding the formation method, when HD and LA-plate were compared, the use of LA-plate reported a significant statistical difference with respect to HD method, with an 85% and 77% respectively (figure 3(a)). Additionally, t-statistic showed statistical significance when HA and LA-plate methods were compared, with an increase in mean spheroid diameter from 180 to 280 µm when LA-plate is used (figure 3(b)). On the other hand, manual spheroid formation in LA-plate reported more homogeneous size than those generated with the HD method.

3.2. Automatized spheroid formation

To allow scalability spheroid formation was automatized using an extrusion 3D bioprinter. To select the appropriate culture plate, 3D bioprinting was performed using both HD method and LA-plate (figure 1(b)). Automatization of spheroid formation process showed an increase in formation efficiency for both methods, with respect to the manual methodology (figure 3(a)). While formation efficiency using LA-plate increased a 15% when the 3D bioprinter was used, formation efficiency increased a 4% for HD method. Despite these results, no statistical differences were found in formation efficiency when the manual and the automatized methodologies were compared for both HD and LA-plate. Nonetheless, when using 3D bioprinting, formation efficiency of HD showed statistically difference to that of LA-plate, with an 80% and 98% respectively. Moreover, formation efficiency distribution was wider for manual spheroid formation (for both HD and LA-plate) than those of the automatized methodology.

Regarding spheroid morphology, spheroid size of manual and automatized methods showed significant differences, with wider size distribution in diameter values that ranged from 100 to 350 µm in the later for both HA and LA-plate (figure 3(b)).

From this point on, all the experiments were carried out using LA-plate to proceed with the rest of studies.

To select the appropriate bioprinting parameters, the effect that feed rate (6–9 well min^{-1}) has on spheroid size was characterized and compared to the spheroids generated manually, using in both cases LA-plate. While bioprinting method significantly increased spheroid diameter when compared to manually generated spheroids, no differences in size were found at both printing velocities (figure 4(a)). Despite this result, spheroid size at lower printing velocities showed a wider distribution in size, with the presence of spheroids with a mean size around 240 µm. This result was supported by the analysis of spheroid size with time (figure 4(b)), which exhibit small-size spheroids at the end of the printing process for lower printing velocities. This data also reported a continuous decrease in the size of the spheroid with time. Although present in both manual and automatized generation methods, decrease in size was more pronounced at 3D bioprinting. ANCOVA test revealed significant differences between printing conditions, with p-value < 0.05.

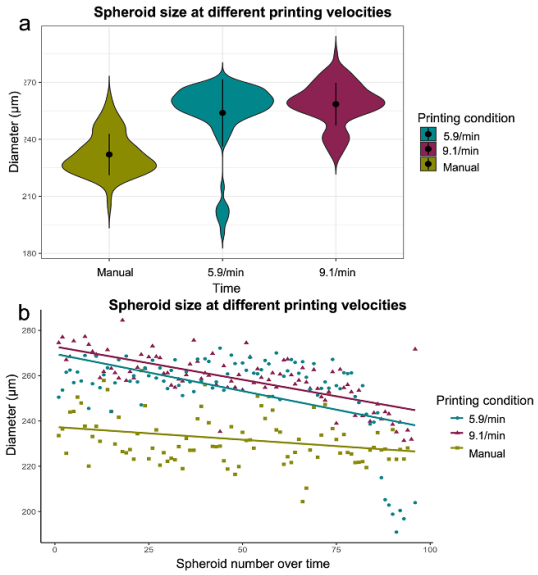

Figure 4. (a) Violin plot representing spheroid size analysis for different printing velocities and (b) scatter plot for the representation of the spheroid size over time for different feed rates (6 and 9 well min^{-1}). Statistical significance: p-value < 0.05*, p-value < 0.01** and p-value < 0.001***.

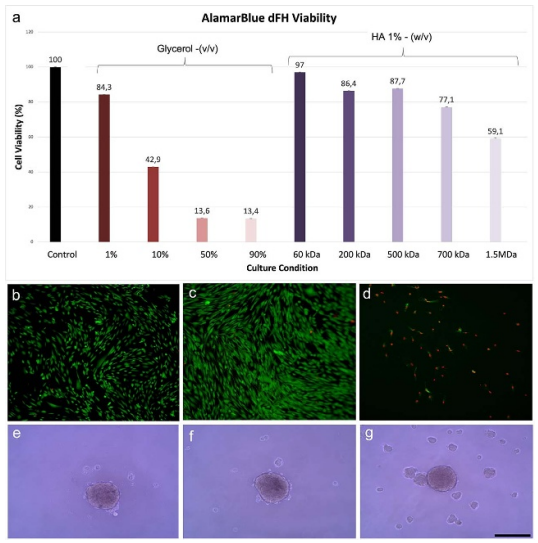

Figure 5. dFH viability results using (a) AlamarBlue and Live/Dead method for (b) control, (c) HA 200 kDa and (d) glycerol 50%. Spheroid morphology after manual generation of the spheroids using HA 500 kDa viscosity enhancer at (e) 0.1%, (f) 0.4% and (g) 0.8% (w/v). Scale bar: 500 µm.

3.2.1. Automatized spheroid formation using viscosity enhancer solutions

To avoid cell sedimentation, both HA and glycerol were considered for the viscosity enhancer solution. First, the effect of glycerol concentration and HA molecular weight on cell viability was analyzed. AlamarBlue test revealed a cell viability below 50% for glycerol concentrations above 1% (figure 5(a)). On the other hand, this test showed that cell viability decreases as the HA molecular weight increased. These results were supported by the Live/Dead assay, in which the number of alive cells present is higher for cell cultures containing HA when compared to those containing glycerol (figures 5(b)–(d)). Viability quantification of the Live/Dead analysis reported a cell viability of 90% for all HA molecular weights and for lower glycerol concentrations, which drops to 0% viable cells for concentrations above 50% (supplementary 2).

Based on viability results, HA of molecular weights of 60, 200 and 500 kDa were selected as potential candidates to be used as viscosity enhancers. In order to select the correct viscosity enhancer concentration, HA at a final concentration of 0.1%, 0.4% and 0.8% (w/v) was used to manually generate cellular spheroids. Visual inspection of the spheroids showed that at highest HA concentrations the spheroids did not correctly form, being surrounded by small cell aggregations (figure 5(g)), while this effect was much less pronounced at 0.1% and 0.4% concentrations (figures 5(e) and (f)). Considering that 0.1% (w/v) solutions showed similar viscosity values than bioinks without any viscosity enhancer (figure 7(b)), 0.4% (w/v) was chosen for bioprinting purposes.

Based on this result and to analyze the effect of viscosity enhancer solution during the bioprinting process, 0.4% (w/v) HA solutions for 60, 200 and 500 kDa molecular weights were used to generate dHF spheroids containing 3000 cells. As a control, the process was repeated in the absence of any viscosity enhancer.

Morphometric analysis of the spheroid showed a statistically significant increase in spheroid size with bioprinting technique that increases in the presence of a viscosity enhancer (figure 6(a)). However, spheroid size distribution within the experiment was reduced in the presence of viscosity enhancer solutions. On the other hand, spheroid roundness was also affected by bioprinting techniques (figure 6(b)), as it decreased and showed a wider distribution within experiment as the molecular weight of the viscosity enhancer increased.

Finally, the effect of viscosity enhancer solutions in cell sedimentation during the bioprinting process was analyzed in terms of spheroid size over time (figure 7(a)). While the spheroid size was reduced a 20% during the printing process in the absence of viscosity enhancer, this trend was reduced in the presence of 0.4% HA for all the molecular weight, showing a homogeneous distribution of spheroid size over time. This result was supported by the ANCOVA analysis (supplementary 3), which reported a significant different in spheroid size over time in the presence of a viscosity enhancer when compared to control conditions. Nonetheless, no statistically significant differences were found neither in spheroid size between different HA molecular weights (supplementary 3), nor in formation efficiency at different printing conditions (supplementary 4).

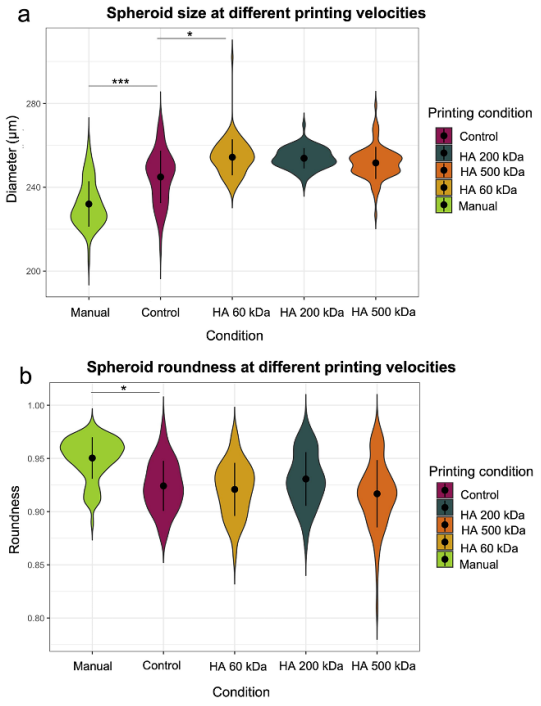

Figure 6. Violin plot representing spheroid morphogenic analysis for different concentration of viscosity enhancer: (a) spheroid size and (b) spheroid roundness. Statistical significance: p-value < 0.05*, p-value < 0.01** and p-value < 0.001***. Control states for bioprinting fabrication without viscosity enhancer.

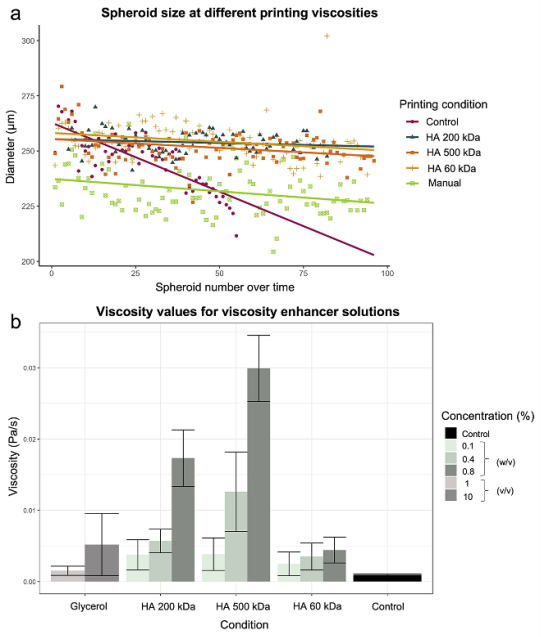

Figure 7. (a) Scatter plot for the representation of the spheroid size over time using different viscosity enhancers. Control states for bioprinting fabrication without viscosity enhancer and (b) viscosity values within the first decade for HA and glycerol solutions at different concentrations.

4. Discussion

The use of cellular spheroids to closely resemble physicochemical *in vivo* conditions and architecture of different cell types has emerged as a promising culture system [1]. This is the case of dHFs, used for the generation of dermal models for drug testing and to accelerate wound healing [9–11]. Recent efforts have been made to refine, standardize, and simplify 3D spheroid culture protocols, as well as the tools required to extract valuable insight from them. Thus, 3D models ought to address the need for mimicking native microenvironment while allowing for a straightforward and user-friendly access to the biological information that they provide [43]. The most relevant spheroid cultures include HD method and U-shape LA-plates due to their simplicity and low price, being widely use in the literature and object of study in this work. When spheroid fabrication was analyzed in terms of formation efficiency, LA-plate postulates as the most efficient method (figure 3(a)), being the reason why it is one of the preferred methods in the literature [11–13, 44]. In terms of morphology, spheroids generated using LA-plate significantly increased their size when compared to those using HD, as a consequence of the reduction of cell compaction (figure 3(b)). This effect, far from being detrimental, may positively improve cell viability, one of the main drawbacks of this culture system [2, 15, 45]. Although the presence of AB and AM has been highlighted to negatively affect spheroid formation efficiency [35], this effect has not been reported in this study neither in formation efficiency or spheroid size (figure 2). This finding becomes very relevant when culturing primary cells, as it takes prolonged periods of time, being much more difficult without AB-AM due to the increased possibility of cell culture contamination. The high reproducibility reported by LA-plates led us to stablish its use using culture medium with AB-AM as the optimal culture conditions for manual spheroid generation.

The most relevant techniques available for high-throughput production of cellular spheroids include: bioreactors, microfluidic devices, and additive manufacturing (3D bioprinting) [9, 16, 46]. While the first method does not guarantee precise control of spheroid size, the second is advantageous in situations that require system miniaturization and precise control of fluid elements. This work sets the focus onto automating and refining culture protocols to attain large-scale spheroid formation and compensate for their laborious nature. 3D bioprinting, particularly extrusion-based bioprinting, potentially contributes to the increase in production and standardization—when compared to microfluidic devices and bioreactors—by automatically seeding the cell solution into each U-shaped well in a precise and human-error-free fashion. Chi-squared analysis showed a statistically significant increase of formation efficiency in both HD and LA-plate methods, reaching this last one almost 100% (figure 3(a)), reason why it was chosen as the preferred culture system for automatized spheroid formation and

proceed with the rest of studies. Nonetheless, when spheroids were generated using this method, they showed a wider distribution in size when compared to the manual loading (figure 3(b)). This effect was explained by a continuous reduction in spheroid size with time that is present for different printing velocities (figure 4(b)). During fabrication, cells were considered as a fundamental and indispensable constituent of the bioink solution, along with cell culture medium providing oxygen and nutrients to the cells. Nonetheless, gravity-driven cell sedimentation within the extrusion syringe [47], arose as a limitation. During manual loading, cell suspension was on continuous mixing with the pipet prior to cell deposition onto each well, ensuring solution homogeneity along time. However, this was not the case during printing conditions, as bioink was loaded in the extrusion syringe. Due to this limitation, viscosity enhancer solutions were considered to supplement the bioinks to reduce cell sedimentation. To increase bioink viscosity different biomolecules have been explored, including HA and glycerol [23]. HA is a biopolymer which belongs to the family of glycosaminoglycans which aims to alter the rheology of the extruded bioink solution by procuring shear-thinning characteristics to it, thus protecting cells from damaging stresses and retaining shape upon printing [48, 49]. Non-crosslinked HA constitutes the safe choice to ensure removal from the construct after printing, being used in the literature in concentrations below 1% (w/v) as a viscosity enhancer [23, 37]. On the other hand, glycerol is a polyalcohol compound with a limited miscibility with water [50], rising as a powerful candidate for enhancing the viscosity of extruded bioinks, since its removal upon printing process completion would only require rinsing with water being use in laser induce forward transfer to increase viscosity of the medium [34]. Despite HA viability results were around 90% in Live/Dead assay (supplementary 2), AlamarBlue showed a decrease in viability as the molecular weight increase (figure 5(a)), and only those above 80% viability (60, 200 and 500 kDa) were chosen. On the contrary, only 1% and 10% (v/v) glycerol solutions exhibited a viability above 80%, being this last one of around 40% in the metabolic analysis (supplementary 2 and figure 5(a)). On account to this result and due to the low viscosity value provided by 1% glycerol solution and the associated problems with its use in cell cultures [51], HA was chosen as viscosity enhancer for bioprinting purposes. Nevertheless, other biomaterials such as fibrinogen or gelatin may be explored as potential viscosity enhancers [23].

Spheroid fabrication for different viscosities report formation efficiency values above 90% with not significantly differences to those of manual loading (supplementary 4). Nonetheless, the increase in size may be explained by the presence of the viscosity enhancer, that reduce cell seeding and compaction within the well (figure 6(a)). Similarly, and due to the same effect, spheroid roundness was affected by the presence of HA in the bioink [37], as they showed a wider distribution on spheroid roundness with increasing molecular weights (figure 6(b)). Regarding cell sedimentation effect, ANCOVA analysis reported significant differences in spheroid size with time in the presence of viscosity enhancer when compared to conventional printing (figure 7(a)). Moreover, as a consequence of sedimentation effect, after spheroid number 50, spheroid size was below 200 μm. While not significantly differences were shown by ANCOVA test at different viscosities (supplementary 3), bioprinting process using 0.4% (w/v) HA 60 kDa showed a horizontal trend closer to that of manual loading. This finding together with the fact that at higher viscosities values spheroid size and roundness were affected because affect cell compaction, led us to choose 0.4% (w/v) HA 60 kDa as the suited printing conditions to avoid cell sedimentation without compromising correct spheroid formation.

5. Conclusion

Spheroid culture systems represent a leap forward in scientific research as they replicate native *in vivo* microenvironments in an *in vitro* scenario with higher degree of accuracy and reliability as compared to conventional monolayer 2D cultures. Pellet culture spheroid formation constitutes an inexpensive and simple yet laborious procedure which procures low quantity of spheroids in a highly user-dependent way. In this study, U-shaped LA-plate arose as a reproducible and scalable procedure for spheroid generation. Moreover, thanks to extrusion-based bioprinting techniques, this process can be further automatized, increasing scalability while reducing errors and operational costs. Besides, homogeneity in the fabrication process was achieved by the addition of HA as overcoming cell sedimentation problems during the printing procedure. The proposed methodology arose as an easy to operate, cheap and reliable way for the scalable production of cellular spheroids.

Data availability statement

All data that support the findings of this study are included within the article (and any supplementary files).

Acknowledgments

We kindly thank Daniel García for their guidance with the rheological experiments. This work was supported by Programa de Actividades de I + D entre Grupos de Investigación de la Comunidad de Madrid, S2018/ BAA-4480, Biopieltec-CM, Programa Estatal de I + D + i Orientada a los Retos de la

Sociedad, RTI2018-101627-B-I00 and Cátedra Fundación Ramón Areces. The experimental techniques used during this study were performed in the Clean-Rooms of Bioengineering, Universidad Carlos III de Madrid, Madrid, Spain.

ORCID iD

Diego Velasco https://orcid.org/0000-0002-1531-1595

References

[1] Achilli T-M, Meyer J and Morgan J R 2012 Advances in the formation, use and understanding of multi-cellular spheroids *Expert Opin. Biol. Ther.* **12** 1347–60
[2] Ryu N-E, Lee S-H and Park H 2019 Spheroid culture system methods and applications for mesenchymal stem cells *Cells* **8** 1620
[3] Friedrich J, Seidel C, Ebner R and Kunz-Schughart L A 2009 Spheroid-based drug screen: considerations and practical approach *Nat. Protocols* **4** 309–24
[4] Liu W, Wang J-C and Wang J 2015 Controllable organization and high throughput production of recoverable 3D tumors using pneumatic microfluidics *Lab Chip* **15** 1195–204
[5] Pampaloni F, Reynaud E G and Stelzer E H K 2007 The third dimension bridges the gap between cell culture and live tissue *Nat. Rev. Mol. Cell Biol.* **8** 839–45
[6] Lin R-Z and Chang H-Y 2008 Recent advances in three-dimensional multicellular spheroid culture for biomedical research *Biotechnol. J.* **3** 1172–84
[7] Shen H, Cai S, Wu C, Yang W, Yu H and Liu L 2021 Recent advances in three-dimensional multicellular spheroid culture and future development *Micromachines* **12** 96
[8] Mehta G, Hsiao A Y, Ingram M, Luker G D and Takayama S 2012 Opportunities and challenges for use of tumor spheroids as models to test drug delivery and efficacy *J. Control. Release* **164** 192–204
[9] Chen Z, Kheiri S, Gevorkian A, Young E W K, Andre V, Deisenroth T and Kumacheva E 2021 Microfluidic arrays of dermal spheroids: a screening platform for active ingredients of skincare products *Lab Chip* **21** 3952–62
[10] Rescigno F, Ceriotti L and Meloni M 2021 Extra cellular matrix deposition and assembly in dermis spheroids *Clin. Cosmet. Invest. Dermatol.* **14** 935–43
[11] Kim S-W, Im G-B, Jeong G-J, Baik S, Hyun J, Kim Y-J, Pang C, Jang Y C and Bhang S H 2021 Delivery of a spheroids-incorporated human dermal fibroblast sheet increases angiogenesis and M2 polarization for wound healing *Biomaterials* **275** 120954
[12] Hu S, Li Z, Cores J, Huang K, Su T, Dinh P-U and Cheng K 2019 Needle-free injection of exosomes derived from human dermal fibroblast spheroids ameliorates skin photoaging *ACS Nano* **13** 11273–82
[13] Lee W J, Song S Y, Roh H, Ahn H M, Na Y, Kim J, Lee J H and Yun C O 2018 Profibrogenic effect of high-mobility group box protein-1 in human dermal fibroblasts and its excess in keloid tissues *Sci. Rep.* **8** 8434
[14] Fennema E, Rivron N, Rouwkema J, van Blitterswijk C and de Boer J 2013 Spheroid culture as a tool for creating 3D complex tissues *Trends Biotechnol.* **31** 108–15
[15] Cui X, Hartanto Y and Zhang H 2017 Advances in multicellular spheroids formation *J. R. Soc. Interface* **14** 20160877
[16] Decarli M C *et al* 2021 Cell spheroids as a versatile research platform: formation mechanisms, high throughput production, characterization and applications *Biofabrication* **13**
[17] Foty R 2011 A simple hanging drop cell culture protocol for generation of 3D spheroids *J. Vis. Exp.* 2720
[18] Timmins N E and Nielsen L K 2007 Generation of multicellular tumor spheroids by the hanging-drop method *Methods Mol. Med.* **140** 141–51
[19] Tung Y-C, Hsiao A Y, Allen S G, Torisawa Y, Ho M and Takayama S 2011 High-throughput 3D spheroid culture and drug testing using a 384 hanging drop array *Analyst* **136** 473–8
[20] Bresciani G, Hofland L J, Dogan F, Giamas G, Gagliano T and Zatelli M C 2019 Evaluation of spheroid 3D culture methods to study a pancreatic neuroendocrine neoplasm cell line *Front. Endocrinol.* **10** 682
[21] Koudan E V *et al* 2020 Multiparametric analysis of tissue spheroids fabricated from different types of cells *Biotechnol. J.* **15** e1900217
[22] Gao C, Lu C, Jian Z, Zhang T, Chen Z, Zhu Q, Tai Z and Liu Y 2021 3D bioprinting for fabricating artificial skin tissue *Colloids Surf.* B **208** 112041
[23] Kang H-W, Lee S J, Ko I K, Kengla C, Yoo J J and Atala A 2016 A 3D bioprinting system to produce human-scale tissue constructs with structural integrity *Nat. Biotechnol.* **34** 312–9
[24] Datta P, Dey M, Ataie Z, Unutmaz D and Ozbolat I T 2020 3D bioprinting for reconstituting the cancer microenvironment *npj Precis. Oncol.* **4** 18
[25] Zhuang P, Chiang Y-H, Fernanda M S and He M 2021 Using spheroids as building blocks towards 3D bioprinting of tumor microenvironment *Int. J. Bioprinting* **7** 444
[26] Goulart E *et al* 2019 3D bioprinting of liver spheroids derived from human induced pluripotent stem cells sustain liver function and viability *in vitro Biofabrication* **12** 015010
[27] Kang Y, Datta P, Shanmughapriya S and Ozbolat I T 2020 3D bioprinting of tumor models for cancer research *ACS Appl. Bio Mater.* **3** 5552–73
[28] Hakobyan D, Médina C, Dusserre N, Stachowicz M-L, Handschin C, Fricain J-C, Guillermet-Guibert J and Oliveira H 2020 Laser-assisted 3D bioprinting of exocrine pancreas spheroid models for cancer initiation study *Biofabrication* **12** 35001
[29] Kingsley D M, Roberge C L, Rudkouskaya A, Faulkner D E, Barroso M, Intes X and Corr D T 2019 Laser-based 3D bioprinting for spatial and size control of tumor spheroids and embryoid bodies *Acta Biomater.* **95** 357–70
[30] Dani S *et al* 2021 Homogeneous and reproducible mixing of highly viscous biomaterial inks and cell suspensions to create bioinks *Gels* **7**
[31] Xu H, Zhang Z and Xu C 2019 Sedimentation study of bioink containing living cells *J. Appl. Phys.* **125** 114901
[32] Mobaraki M, Ghaffari M, Yazdanpanah A, Luo Y and Mills D K 2020 Bioinks and bioprinting: a focused review *Bioprinting* **18** e00080
[33] Hauptstein J *et al* 2020 Hyaluronic acid-based bioink composition enabling 3D bioprinting and improving quality of deposited cartilaginous extracellular matrix *Adv. Healthcare Mater.* **9** e2000737
[34] Deng Y, Renaud P, Guo Z, Huang Z and Chen Y 2017 Single cell isolation process with laser induced forward transfer *J. Biol. Eng.* **11** 2
[35] Higgins C A, Itoh M, Inoue K, Richardson G D, Jahoda C A B and Christiano A M 2012 Reprogramming of human hair follicle dermal papilla cells into induced pluripotent stem cells *J. Invest. Dermatol.* **132** 1725–7
[36] Topouzi H, Logan N J, Williams G and Higgins C A 2017 Methods for the isolation and 3D culture of dermal papilla cells from human hair follicles *Exp. Dermatol.* **26** 491–6
[37] Horder H *et al* 2021 Bioprinting and differentiation of adipose-derived stromal cell spheroids for a 3D breast cancer-adipose tissue model *Cells* **10** 803
[38] M'Barki A, Bocquet L and Stevenson A 2017 Linking rheology and printability for dense and strong ceramics by direct ink writing *Sci. Rep.* **7** 6017

[39] McHugh M L 2013 The chi-square test of independence *Biochem. Med.* **23** 143–9
[40] Gudgeon A C and Howell D C 1994 Statistical methods for psychology *Statistician* **43** 211
[41] Wildt A R and Ahtola O 1978 *Analysis of Covariance* (SAGE Publications, Inc.) (https://doi.org/10.4135/9781412983297)
[42] Surbhi S 2017 Difference between ANOVA and ANCOVA (available at: https://keydifferences.com/difference-between-anova-and-ancova.html)
[43] Griffith L G and Swartz M A 2006 Capturing complex 3D tissue physiology *in vitro Nat. Rev. Mol. Cell Biol.* **7** 211–24
[44] Arai K, Murata D, Takao S, Verissiomo A R and Nakayama K 2020 Cryopreservation method for spheroids and fabrication of scaffold-free tubular constructs *PLoS One* **15** e0230428
[45] Cesarz Z and Tamama K 2016 Spheroid culture of mesenchymal stem cells *Stem Cells Int.* **2016** 9176357
[46] Behroodi E, Latifi H, Bagheri Z, Ermis E, Roshani S and Salehi Moghaddam M 2020 A combined 3D printing/CNC micro-milling method to fabricate a large-scale microfluidic device with the small size 3D architectures: an application for tumor spheroid production *Sci. Rep.* **10** 22171
[47] Unagolla J M and Jayasuriya A C 2020 Hydrogel-based 3D bioprinting: a comprehensive review on cell-laden hydrogels, bioink formulations, and future perspectives *Appl. Mater. Today* **18**
[48] Shin J H and Kang H-W 2018 The development of gelatin-based bio-ink for use in 3D hybrid bioprinting *Int. J. Precis. Eng. Manuf.* **19** 767–71
[49] Highley C B, Rodell C B and Burdick J A 2015 Direct 3D printing of shear-thinning hydrogels into self-healing hydrogels *Adv. Mater.* **27** 5075–9
[50] Egorov G I, Makarov D M, Egorov G I and Makarov D M 2014 Volumetric properties of binary liquid-phase mixture of (water + glycerol) at temperatures of (278.15 to 323.15) K and pressures of (0.1 to 100) MPa *J. Chem. Thermodyn.* **79** 135–58
[51] Cunha C C, Arvelos L R, Costa J O and Penha-Silva N 2007 Effects of glycerol on the thermal dependence of the stability of human erythrocytes *J. Bioenerg. Biomembr.* **39** 341–7